Electronic Supplementary Information

MWCNT Synergy for Boosting Electrochemical Kinetics of V_2O_5 Cathode for Lithium-ion Battery

Hamna Mustafa[a,i], Yanlong Yu[b], Amina Zafar[a,c], Yanguo Liu[d], Shafqat Karim[a], Saqib Javed[e], Sheeraz Mehboob[f], Hongyu Sun[d], Shafqat Hussain[a], Atta Ullah Shah[g], Syed Zahid Hussain[h], Amna Safdar[i,*], Amjad Nisar[a,*] and Mashkoor Ahmad[a,*]

[a]*Nanomaterials Research Group, Physics Division, PINSTECH, Islamabad 44000, Pakistan.*

[b]*College of Chemistry and Chemical Engineering, Northeast Petroleum University, Daqing, 163318, PR China.*

[c]*Central Analytical Facility Division, PINSTECH, Islamabad 44000, Pakistan.*

[d]*School of Resources and Materials, Northeastern University at Qinhuangdao, Qinhuangdao, 066004, PR China.*

[e]*Theoretical Physics Division, PINSTECH, Islamabad 44000, Pakistan*

[f]*Chemistry Division, PINSTECH, Islamabad 44000, Pakistan*

[g]*National Institute of Lasers and Optronics College, Pakistan Institute of Engineering and Applied Sciences, Nilore, Islamabad 45650, Pakistan*

[h]*Materials Division, PINSTECH, Islamabad 44000, Pakistan*

[i]*School of Chemical and Materials Engineering National University of Sciences and Technology (NUST), Islamabad 44000, Pakistan.*

Correspondence Email: mashkoorahmad2003@yahoo.com (Mashkoor Ahmad)

2. Experimental

2.1 Reagents and materials

Vanadium pentoxide (V_2O_5) powder, multiwalled carbon nanotubes (MWCNT's) and graphite flakes were purchased from Sigma Aldrich. Hydrogen peroxide solution (H_2O_2) was obtained from Honey well. Sodium nitrate ($NaNO_3$) and potassium permanganate ($KMnO_4$) were purchased from Riedel-de Haën. Ethanol was received from AnalaR. Sulphuric acid (H_2SO_4) and Hydrochloric acid (HCl) were supplied by MERCK (E.Merck, Darmstadt, F. R. Germany). Deionized water was used throughout the synthesis and measurements.

2.1 Synthesis of V_2O_5

V_2O_5precursor powder (0.455 g) was dissolved in deionized water (37.5 mL) at room temperature and then H_2O_2 (6.25 mL) was added and kept continuously stirred for 30 min. The resultant solution was transferred to a Teflon lined autoclave (50 mL) and kept in an oven at 205 ^oC for 3 days. The product was washed with ethanol and DI water several times to remove the impurities. The sample was dried at 80 ^oC in vacuum for 6 h and then annealed in air at 500 ^oC for 2 h. The annealed sample was then grinded finely into the fine powder[1].

2.3 Synthesis of GO and rGO

The synthesis of GO was carried out using a modified Hummers method as we have previously reported[2]. Briefly, 2g graphite flake and $NaNO_3$ was mixed in 90 ml of sulphuric acid (H_2SO_4) and stirred for 2 hours while keeping the temperature less than 5 ^oC. Then 12 g of potassium permanganate was added to the reaction mixture slowly, maintaining the temperature at or below 15^oC to avoid the explosion and allow magnetic stirring for 30 mins. After that, 184 ml of water was poured very carefully to dilute the mixture because of the exothermic reaction. After addition of water the ice bath was removed from reaction while continuing the stirring for further 2 hours. The temperature reaches to 35^oC. The mixture was kept in a reflux-system at 98^oC for the 10-15 mints. After 10 minutes, the temperature was changed to 30 ^oC which resulted in brown colored solution. Then reaction was cooled down to room temp at 25^oC and stirred the reaction mixture for next 2 hours. 30% of H_2O_2 (40 ml) and 160 ml of hot water was added into the solution, and the solution was stirred for 1 hour. Mixture was left for overnight in an open air at room

temperature. The product blend was then moved to the sonic bath and ultra-sonicated for 35minutes. To remove the impurities, the product was washed several times with ethanol, DI-water and with 10% of HCl. Gel like substance was obtained after centrifuge which was further dried in oven for 24 hours. The obtained GO was then finely grinded into the fine powder. The powder was then assembled into the alumina ceramic crucible and covered with the lid. To anneal the sample this crucible was then placed inside the muffle furnace for 1 h at 500 ^{o}C. The final product was then stored in the glass reagent bottle for further use.

2.4 Synthesis of V_2O_5/carbon-based hybrid systems

The hybrid nanomaterials including V_2O_5/MWCNT's and V_2O_5/rGO were prepared by a facile hydrothermal method as reported [3]. MWCNT's and rGO were taken about 10% weight ratio of V_2O_5.The chosen amount of MWCNT's were dispersed into 20 mL of deionized water and ultrasonicated for 45 min. Subsequently, 2mL of acetic acid was added. After stirring for 10 min, 10mL of the prepared solution of annealed V_2O_5 was added drop by drop in the above solution. After stirring for 30 min in the room temperature, the resultant solution was transferred into a sealed Teflon container and kept in an electrical oven at 200 ^{o}C for 3h. The precipitates obtained after hydrothermal treatment were filtered and washed several times with pure ethanol and deionized water and dried for 24h at 60 ^{o}C.

2.5 Material Characterization

The morphology and chemical composition of the samples were studied by field- emission scanning electron microscopy (FE-SEM, TESCAN MIRA A-3) equipped with an energy dispersive X-ray (EDX) system and high transmission electron microscope (TEM, JEOL JEM-2100 F, 200 kV). The Raman spectrum was recorded from 100 to 1800 cm^{-1}by using Horiba Xplora microscope at 532nm laser. Structural properties of the samples were examined using Bruker Model D8 Advance X-ray powder diffractometer (XRD) in the diffraction angle range 5-80°with Cu-Kα radiation (λ = 1.54060 Å). Fourier transform infrared spectroscopy (FTIR) was recorded on KBr pallets in the range of 400-4000 cm^{-1} by using a Nicolet iS5o-FTIR spectrometer. The surface composition and valance-state were determined by X-ray photo-electron spectroscopy (XPS; Super ESCA beam at Electra, Trieste, Italy).

2.6 Battery assembly and performance measurements

The working electrode was prepared by dispersing active material, carbon black and soft binder PVDF (polyvinylidene fluoride) in NMP (N-methylpyrrolidone) solvent with a weight ratio of 70:20:10. The slurry was spread on aluminum foil disks and dried in a vacuum oven at 60 ^{o}C overnight then cut into disks (diameter 15nm). The cells were assembled in an Ar-filled glovebox using lithium foil as negative electrode, porous polypropylene as the separator, and 1M $LiPF_6$ in ethylene carbonate, dimethyl carbonate and ethylene methyl carbonate (2:1:2 by volume) was used as the electrolyte. For determining electrochemical performance, galvanostatic charge/discharge tests with various current densities, each for 10 cycles were performed using 8 Channel Battery Analyzer system (BTS8) in the voltage range of 1.5 4.0 V (vs.Li/Li^+). Cyclic voltammogram (CV; 1.5-4.2V, 0.0005 mVs^{-1}) measurements were performed by using a LAND cell-testing system and CHI660C (Chenghua, Shanghai) electrochemical workstation. The electrochemical impedance spectroscopy (EIS) measurements were collected using CHI660C electrochemical workstation with amplitude of 5 mV in the frequency range from 100 kHz to 0.01Hz.

2.7 Computational details

In this study, all calculations have been performed by employing planewave pseudopotential approach as implemented in VASP[4]. Generalized gradient approximation (GGA) with Perdew–Burke–Ernzerhof (PBE) parameterization was used as exchange correlation functional [5], though results for electronic structure were further corrected by using hybrid HSE06 method. A kinetic energy cut-off of 500 eV was employed while convergence criteria of total energy and forces were set to 10^{-5} eV and 0.01 eV/Å, respectively. In order to model MWCNT, we have employed (4,4)@ (8,8)@ (12,12) three wall multi carbon nanotube. The calculated work function was 4.22 eV, in good agreement with the experimental value of 4.30[6]. The calculations were also performed with larger tube ((8,8)@ (12,12)@ (16,16)), though change in work function remained negligible, highlighting the convergence of results. For orthorhombic V_2O_5, energetically optimum surface was employed which is obtained by cleaving layers bonded by weak van der Waals bonds [7]. Specifically, two layers were utilized which were sufficient to obtain converged results. In order to provide energy level alignment at V_2O_5/MWCNT interface, energy levels of V_2O_5 and MWCNT were calculated separately with respect to vacuum level. This approach is reasonable since

interaction between V_2O_5 and MWCNT should be relatively weak due to geometry of MWCNT while a combined study of V_2O_5/MWCNT interface would be computationally prohibitive. We note that this approach is routinely employed to estimate efficiency and direction of interfacial charge transfer within electronic devices[8,9].

3. Results and discussion

3.1 Compositional analysis of V_2O_5 and V_2O_5 based hybrid composites by FTIR

FTIR analysis was carried out to investigate the chemical composition and bond analysis of V_2O_5 and V_2O_5 based hybrid composites including V_2O_5/MWCNT's and V_2O_5/rGO as shown in Fig. S3. The vibrational band at 462 cm^{-1} corresponds to the stretching absorption peak of triply coordinated oxygen atom between three vanadium atoms [10]. The peaks at 834 and 521 cm^{-1} correspond to asymmetric and symmetric stretching of V–O–V bridge. The band located at 622 cm^{-1} assigned to the vanadyl stretching mode (e.g. δV–O).The characteristics band at 1020 cm^{-1} is ascribed to stretching vibration of terminal oxygen bonds (V=O) [11–13]. Thus, the characteristic peaks ranging from 1020-462 cm^{-1} confirms the bonding structure of the vanadate. In the spectra of V_2O_5/rGO, the band at 1139 cm^{-1} is attributed to the presence of C-O stretching. It shows that the stretching vibration of C-OH and C=O bonds in rGO disappears which proves that the GO material has been reduced successfully. In V_2O_5/rGO it is due to the unoxidized graphitic domains whereas in V_2O_5/MWCNT's spectra the vibration represents the graphite structure present in the MWCNT framework which is caused by the five-membered ring or seven membered ring at the turning point or seal of the MWCNTs [14,15]. In both V_2O_5/MWCNT's and V_2O_5/rGO, the band at 1401 cm^{-1} and 1629 cm^{-1} is assigned to the stretching in the sp^2 vibration plane of C=C bond [16,17]. Lastly, the peaks appearing at 3463 cm^{-1} in the spectra of both the hybrids represents the stretching vibrations of hydroxyl group (-OH) or the trapped water [14,16].

References

[1] Y. Yu, J. Li, X. Wang, B. Chang, J. Wang, M. Ahmad, H. Sun, Journal of Colloid and Interface Science Oxygen vacancies enhance lithium storage performance in ultralong vanadium pentoxide nanobelt cathodes, J. Colloid Interface Sci. 539 (2019) 118–125. https://doi.org/10.1016/j.jcis.2018.12.046.

[2] S. Tabassum, S. Naz, A. Nisar, H. Sun, S. Karim, M. Khan, S. Shahzada, A. Rahman, M. Ahmad, and graphene oxide on the performance of, (2019) 18925–18934. https://doi.org/10.1039/c9nj04532e.

[3] X. Liang, G. Gao, Y. Liu, Z. Ge, P. Leng, Carbon nanotubes / vanadium oxide composites as cathode materials for lithium-ion batteries, J. Sol-Gel Sci. Technol. (2017) 224–232. https://doi.org/10.1007/s10971-016-4293-8.

[4] G. Kresse, J. Furthmiiller, Efficiency of ab-initio total energy calculations for metals and semiconductors using a plane-wave basis set av *, Comput. Mater. Sci. 6 (1996) 15–50. https://doi.org/10.1016/0927-0256(96)00008-0.

[5] J.P. Perdew, K. Burke, M. Ernzerhof, Generalized Gradient Approximation Made Simple, Phys. Rev. Lett. 77 (1996) 3865–3868. https://doi.org/10.1103/PhysRevLett.77.3865.

[6] H. Ago, T. Kugler, F. Cacialli, W.R. Salaneck, M.S.P. Shaffer, A.H. Windle, R.H. Friend, Work Functions and Surface Functional Groups of Multiwall Carbon Nanotubes, J. Phys. Chem. B. 103 (1999) 8116–8121. https://doi.org/10.1021/jp991659y.

[7] J. Goclon, R. Grybos, M. and Witko, J. Hafner, Relative stability of low-index V2O5 surfaces : a density functional investigation, J. Phys. Condens. Matter. 21 (2009) 095008 (8pp). https://doi.org/10.1088/0953-8984/21/9/095008.

[8] N.J. Jeon, H. Na, E.H. Jung, T. Yang, Y.G. Lee, G. Kim, H. Shin, S. Il Seok, J. Lee, J. Seo, A fluorene-terminated hole-transporting material for highly efficient and stable perovskite solar cells, Nat. Energy. 3 (2018). https://doi.org/10.1038/s41560-018-0200-6.

[9] Z.-X.X. and G.-J.F. Guang Yang, Yu-Long Wang, Jia-Ju Xu, Hong-Wei Lei, Cong Chen, Hai-Quan Shan, Xiao-Yuan Liu, A Facile Molecularly Engineered Copper (II) Phthalocyanine as Hole Transport Material for Planar Perovskite Solar Cells with Enhanced Performance and Stability, Nano Energy. 31 (2017) 322–330. https://doi.org/10.1016/j.nanoen.2016.11.039.

[10] J. Chu, Z. Kong, D. Lu, W. Zhang, X. Wang, Y. Yu, S. Li, X. Wang, S. Xiong, J. Ma, Hydrothermal synthesis of vanadium oxide nanorods and their electrochromic performance, Mater. Lett. 166 (2016) 179–182. https://doi.org/10.1016/j.matlet.2015.12.067.

[11] R.S. Chen, W.C. Wang, C.H. Chan, H.P. Hsu, L.C. Tien, Y.J. Chen, Photoconductivities in monocrystalline layered V2O5 nanowires grown by physical vapor deposition, Nanoscale Res. Lett. 8 (2013) 1–8. https://doi.org/10.1186/1556-276X-8-443.

[12] N. Pinna, M. Willinger, K. Weiss, J. Urban, R. Schlo, Local Structure of Nanoscopic Materials: V2O5 Nanorods and Nanowires, Nano Lett. 3, No.8 (2003) 1131–1134. https://doi.org/10.1021/nl034326s.

[13] M. Malta, R.M. Torresi, Electrochemical and kinetic studies of lithium intercalation in composite nanofibers of vanadium oxide/polyaniline, Electrochim. Acta. 50 (2005) 5009–5014. https://doi.org/10.1016/j.electacta.2005.05.035.

[14] X. Mu, B. Yuan, X. Feng, S. Qiu, L. Song, Y. Hu, The effect of doped heteroatoms (nitrogen, boron, phosphorus) on inhibition thermal oxidation of reduced graphene oxide, RSC Adv. 6 (2016) 105021–105029. https://doi.org/10.1039/c6ra21329d.

[15] F. Zhou, Y. Wang, W. Wu, T. Jing, S. Mei, Y. Zhou, Synergetic signal amplification of multi-walled carbon nanotubes-Fe3O4 hybrid and trimethyloctadecylammonium bromide as a highly sensitive detection platform for tetrabromobisphenol A, Sci. Rep. 6 (2016) 1–12. https://doi.org/10.1038/srep38000.

[16] J.-U. and M.S.-P. Miller Ruidíaz-Martínez, Miguel A.Álvarez, María Victoria López-Ramón, Guillermo Cruz-Quesada, Hydrothermal Synthesis of rGO-TiO2 Composites as High-Performance UV Photocatalysts for Ethylparaben Degradation, Catalysts. 10 (2020) 520. https://doi.org/10.3390/catal10050520.

[17] S.S. and D.M. Bulkesh, TIO2 / MWCNT NANOCOMPOSITE BASED ELECTRODE FOR DYE SENSITIZED SOLAR CELLS : PREPARATION AND CHARACTERISATION, Int. J. Sci. Technol. Manag. 04 (2015) 98–103. www.ijstm.com.

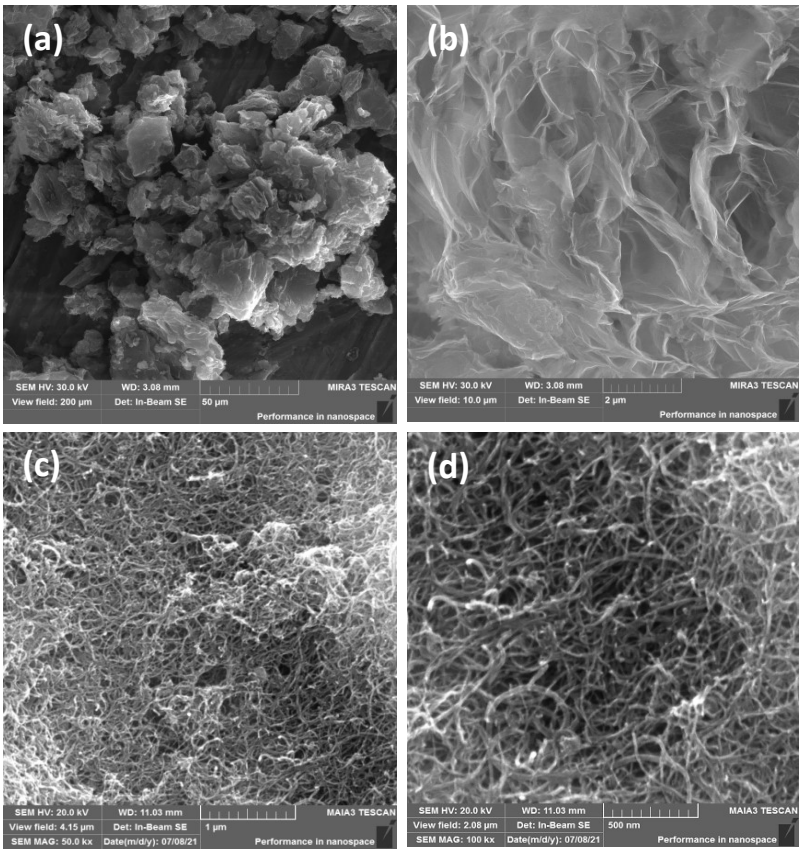

Figure S1. Low and high magnification FESEM images of (a, b) rGO (c, d) MWCNTs.

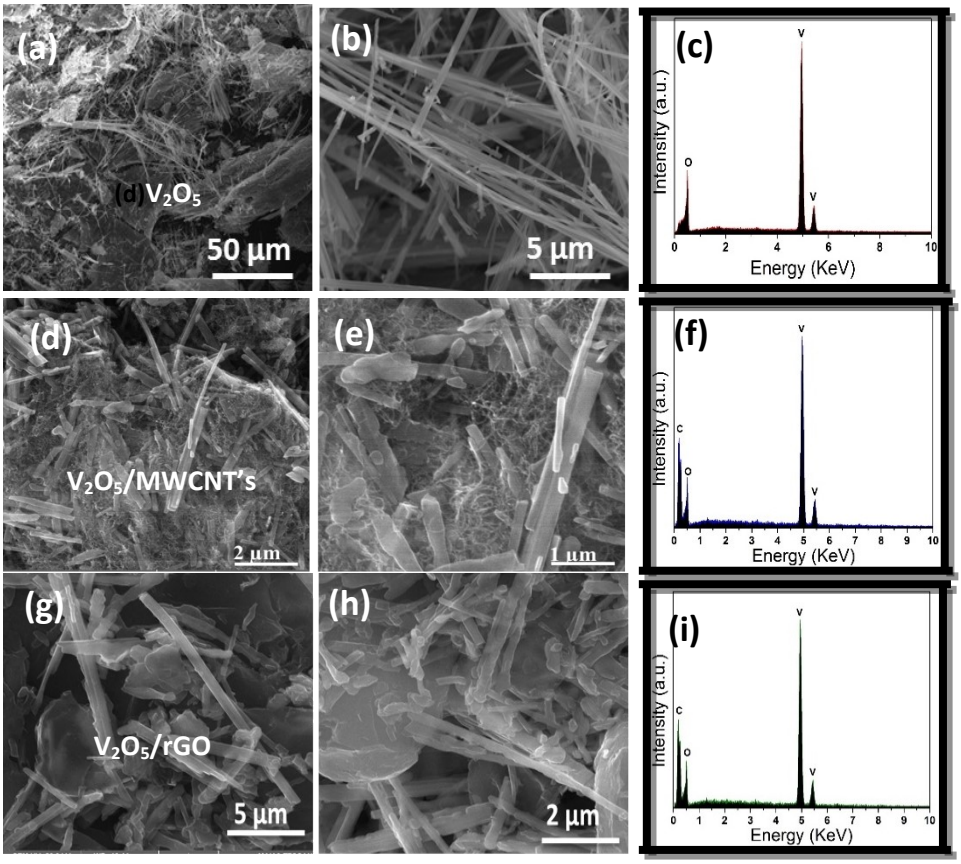

Figure S2. Low and high magnification FESEM images of (a, b) V_2O_5 (d, e) V_2O_5/MWCNTs (g, h) V_2O_5/rGO and corresponding EDX spectrum of (c) V_2O_5 (f) V_2O_5/MWCNTs (i) V_2O_5/rGO respectively.

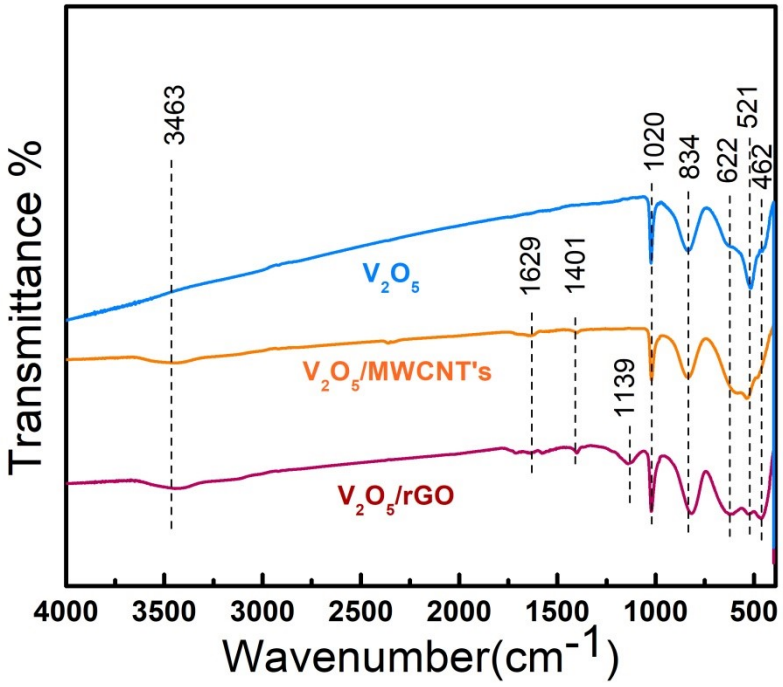

Figure S3. FTIR spectra of V_2O_5, V_2O_5/MWCNTs and V_2O_5/rGO.